The Sign and Magnitude of ^{2h}J(F,F) and ^{1h}J(F,H) in FH···FH. A CLOPPA Analysis of Their Distance Dependence

Claudia G. Giribet* and Martín C. Ruiz de Azúa

Department of Physics, Facultad de Ciencias Exactas y Naturales, University of Buenos Aires, Ciudad Universitaria, Pab. I, (1428) Buenos Aires, Argentina

Received: January 5, 2006; In Final Form: August 11, 2006

The sign change of the intermolecular ^{2h}J(F,F) coupling in the $(HF)_2$ dimer as a function of the F−F distance is discussed by means of the CLOPPA method. It is found that it is due to the competition of positive and negative contributions involving the interaction of the σ lone pair of the acceptor nucleus with vacant molecular orbitals localized in the F−H···F moiety and with other molecular orbitals localized in the donor molecule. The origin of the sign of each contribution is fully determined by analyzing the response of the electronic system to the magnetic perturbation at the acceptor F nucleus. ^{2h}J(F,F) coupling in the FH···F^-, which is positive for all F−F distances, is also analyzed in order to look for the differences with the former case.

Introduction

Spin−spin coupling constants between nuclei across hydrogen bonds have become a valuable tool to detect and characterize hydrogen bonded moieties. From the recent first measurement,[1,2] extensive work has been done in order to study different aspects of this type of couplings from a theoretical point of view.[3−6]

In a recent paper,[7] Del Bene et al. were fully dedicated to analyze the unusual behavior of the ^{2h}J(F,F) coupling for the $(HF)_2$ dimer as a function of the hydrogen bond distance. They found that this coupling does not exhibit the usual behavior of decreasing (in absolute value) with increasing F−F distance. These authors pointed out: "When we plotted the distance- and orientation-dependence of $^{2h}J_{F-F}$ for $(HF)_2$ we found these plots unusual and puzzling. For the first time we observed a change in the sign of the Fermi-contact (FC) term as a function of hydrogen bond distance, and found that neither the FC nor the $^{2h}J_{F-F}$ curve exhibits the usual behavior of decreasing (in absolute value) with increasing F−F distance." Previously, Pecul et al. had studied the $(HF)_2$ dimer[8] and had reported that the ^{2h}J(F,F) coupling presents this peculiar dependence with the F−F distance, different from the expected exponential decay that, for instance, presents the same coupling in FHF^-. This peculiar behavior of the Fermi-contact (FC) term was investigated by means of the NMR triplet wave function (NMRTW) model,[9] which relates the orientation of coupled nuclei to the phases of the excited triplet wave functions that couple to the ground state. Del Bene et al. conclude that the sign of the FC term is the result of the competition of positive and negative contributions from different triplet states. However, the electronic mechanisms that originate this unusual behavior deserve further analysis. In that sense, the CLOPPA method is an adequate tool to provide an interesting and rigorous insight that complements Del Bene's previous study.

The CLOPPA (contributions from localized orbitals within the polarization propagator approach) method, combined with the IPPP (inner projections of the polarization propagator) technique,[10−13] is a useful tool to identify the electronic mechanisms operating in a given phenomenon in terms of localized molecular orbitals. It was implemented at the ab initio level for the theoretical analysis of NMR spin−spin couplings[10−16] and the static molecular polarizability tensor.[17,14,15] This method was applied to study, for instance, one-bond C−H couplings in complex systems with C−H···O interactions,[17] and, very recently, to determine the electronic mechanisms which give rise to ^{1h}J(A,H) and ^{2h}J(A,D) couplings across D−H···A hydrogen bonds in a set of small model compounds. In particular, the problem of the larger absolute value of ^{2h}J(A,D) compared to ^{1h}J(A,H) was also successfully analyzed.[18]

The aim of the present work is to present an alternative insight to analyze the sign change that characterizes the FC term of the ^{2h}J(F,F) coupling across the F−H···F hydrogen bond in the $(HF)_2$ dimer as a function of distance, by means of the CLOPPA method. This approach complements the above-mentioned studies, as the origin of this unusual behavior is analyzed in terms of localized molecular orbitals (LMOs) that closely represent chemical functions like cores, bonds, lone pairs, and the corresponding antibonding orbitals. A CLOPPA analysis of ^{1h}J(F,H) is also presented in order to establish differences with ^{2h}J(F,F). Transmission mechanisms are identified in terms of "coupling pathways" J_{ij} involving two occupied (i,j) localized molecular orbitals, and "coupling pathways" $J_{ia,jb}$ involving two occupied (i,j) and two vacant (a,b) LMOs. The relative importance of different LMOs in the coupling transmission and the role played by each one can then be assessed. In the first place, a brief account of the IPPP−CLOPPA method is presented. Each J_{ij} and $J_{ia,jb}$ coupling pathways are explicitly related to the spin electronic density of an occupied LMO at the site of a given nucleus. In particular, the interpretation of "four indices" coupling pathways in this context is presented for the first time. Numerical results of the IPPP−CLOPPA analysis of ^{1h}J(F,H) and ^{2h}J(F,F) are presented in the Results and Discussion. As an accessory subject, a preliminary discussion about correlation effects is also presented. An "ad hoc" correction to the RPA polarization propagator is proposed, to achieve a better quantitative agreement between RPA and SOPPA values. The sign of the coupling is analyzed following the new interpretation

* Corresponding author. E-mail: giribet@df.uba.ar.

10.1021/jp060095c CCC: $33.50
Published on Web 09/19/2006

of $J_{ia,jb}$. Thus, this sign can be explained in terms of changes in the electronic density of the magnetically perturbed LMOs. As a complement, the analysis of the dependence of the ^{2h}J(F,F) coupling in FH···F− on the F−F distance, which presents the expected exponential decay, is also addressed, to investigate if there is any fundamental difference that account for the unlike behavior between this coupling in $(FH)_2$ and FHF−. Interesting features are found, which complement previous studies.[7,8]

Method

CLOPPA Method. Since the CLOPPA (contributions from localized orbitals within the polarization propagator approach) method was fully described previously,[10−13] only its main ideas are presented here, for the sake of comprehension.

Within the polarization propagator (PP) formalism,[19] any component of the spin−spin coupling constant between nuclei N and M can be expressed as[10]

$$J(N,M) = \Omega \sum_{ia,jb} V_{ia}(N) P_{ia,jb} V_{jb}(M) \tag{1}$$

where Ω is a constant which depends on the interaction considered and contains, among others, the gyromagnetic factors of nuclei N and M; i,j (a,b) indices stand for occupied i,j (vacant a^*, b^*) molecular orbitals (MOs) of a Hartree−Fock reference state; $P_{ia,jb}$ is the PP matrix element connecting "virtual excitations" $i \rightarrow a^*$ and $j \rightarrow b^*$. Equation 1 can be evaluated at different levels of approximation: RPA, SOPPA,[20,21] etc. Within the present implementation, the CLOPPA analysis can be carried out only at the RPA level. $V_{ia}(N)$ represents the matrix element of the perturbative Hamiltonian between MOs i and a^* centered at nucleus N and a similar definition stands for $V_{jb}(M)$. These elements are called "perturbators".

In the CLOPPA method, $J(N,M)$, eq 1, is rewritten in terms of localized MOs (LMOs), by applying to the PP matrix elements and to the perturbators a convenient unitary transformation from canonical HF MOs to occupied and vacant LMOs. These LMOs can be defined in such a way that they represent chemical functions like bonds, lone pairs and atomic inner shells, and their corresponding "anti" LMOs (antibonds, anti-lone pairs, etc.). The formal expression of $J(N,M)$, eq 1, is not altered by the application of this transformation and the only difference is that i,j indices now stand for occupied LMOs and a,b indices stand for vacant LMOs. Thus, $J(N,M)$ can be expressed in terms of four-indices "coupling pathways" which involve two virtual excitations $i \rightarrow a^*$ and $j \rightarrow b^*$:

$$J(N,M) = \sum_{ia,jb} J_{ia,jb} \tag{2}$$

where

$$J_{ia,jb} = \begin{cases} (V_{ia}(N)V_{jb}(M) + V_{jb}(N)V_{ia}(M))P_{ia,jb} & ia \neq jb \\ V_{ia}(N)V_{jb}(M)P_{ia,jb} & ia = jb \end{cases} \tag{3}$$

Within this approach, it is useful to define two-indices terms for a given pair of occupied LMOs i and j (two-indices coupling pathway) by summing over the whole set of vacant LMOs:

$$J_{ij} = \sum_{a,b} J_{ia,jb} \tag{4}$$

As was shown in a previous paper,[18] in the particular case that the perturbative Hamiltonian is a Fermi contact-like operator (FC), two-indices coupling pathways can be written as

$$J_{ij} \propto -\frac{1}{2}\{[|\tilde{\psi}_i^M(N)|^2 - |\psi_i(N)|^2] + [|\tilde{\psi}_j^M(N)|^2 - |\psi_j(N)|^2]\} \tag{5}$$

or, alternatively,

$$J_{ij} \propto -\frac{1}{2}\{[|\tilde{\psi}_i^M(N)|^2 - |\psi_i(N)|^2] + [|\tilde{\psi}_i^N(M)|^2 - |\psi_i(M)|^2]\} \tag{6}$$

where $|\psi_i(N)|^2$is the electronic density of the i LMO at the nucleus N site, and $|\tilde{\psi}_i^M(N)|^2$is the electronic density of the perturbed i LMO at the same site, due to the LMO j perturbed at the M nucleus site, calculated up to second order in V. Similar definitions stand for similar symbols. Equations 5 and 6 allow the following interpretation of the two-indices coupling pathways J_{ij}: (a) the sum of the electronic density changes of LMOs i and j at the site of nucleus N when LMO j and i are perturbed at the other nucleus, respectively; (b) the sum of electronic density changes of LMO i at both nuclei sites when LMO j is perturbed at the other nucleus site.

Taking into account that, within ab initio calculations, there are several vacant LMOs that can be ascribed to each type of local fragment, four-indices coupling pathways can also be defined as

$$J_{ia,jb} = \sum_{\substack{\alpha \in 'a' \\ \beta \in 'b'}} J_{i\alpha,j\beta} \tag{7}$$

where α (β) represent vacant LMOs of the a^* (b^*) type. These four-indices coupling pathways allow a similar interpretation than two-indices ones. Consider an FC-like operator V_{jb}^M which connects the j occupied LMO with the vacant LMOs of the b^*-type at the site of nucleus M:

$$V_{jb}^M = \sum_{\beta}^{b} \langle \beta^* | \delta(\vec{r} - \vec{R}_M) | j \rangle (\beta^+ j + j^+ \beta) = \sum_{\beta}^{b} V_{j\beta}(M)(\beta^+ j + j^+ \beta) \tag{8}$$

where β^+ (β) represents a creation (annihilation) operator which creates (annihilates) an electron in a β LMO. A similar explanation stands for j^+ (j). In the presence of this perturbative operator, the i occupied LMO is modified in such a way that it now has contributions from vacant LMOs. In particular, the contribution of the a^*-type vacant LMOs to the modified $|\tilde{i}_a^M\rangle$ LMO, $|\tilde{i}_a^M\rangle$, can be expressed as

$$|\tilde{i}_a^M\rangle = |i\rangle + \sum_{\alpha \in 'a'} \sum_{\beta \in 'b'} P_{i\alpha,j\beta} V_{j\beta}(M) |\alpha^*\rangle = |i\rangle + \delta |\tilde{i}_a^M\rangle \tag{9}$$

The contribution to the electronic density of the perturbed i LMO at the nucleus N site from the a^*-type vacant LMOs, $|\tilde{\psi}_{ia}^M(N)|^2$, due to the LMO j perturbed at the M nucleus site, results, up to second order in V:

$$|\tilde{\psi}_{ia}^M(N)|^2 = \langle \tilde{i}_a^M | \delta(\vec{r} - \vec{R}_N) | \tilde{i}_a^M \rangle \cong \langle i | \delta(\vec{r} - \vec{R}_N) | i \rangle + 2 \sum_{\alpha \in 'a'} \sum_{\beta \in 'b'} P_{i\alpha,j\beta} V_{i\alpha}(N) V_{j\beta}(M) \tag{10}$$

Taking into account eqs 3, 7, and 10, each $J_{ia,jb}$, eq 7,

is proportional to

$$J_{ia,jb} \propto -\frac{1}{2}\{[|\tilde{\psi}_{ia}^{M}(N)|^2 - |\psi_i(N)|^2] + [|\tilde{\psi}_{jb}^{M}(N)|^2 - |\psi_j(N)|^2]\} \quad (11)$$

where $\psi_i(N)$ is the unperturbed LMO i evaluated at the N nucleus site (similar definitions stand for the other symbols). Following a similar reasoning, $J_{ia,jb}$ can also be expressed as

$$J_{ia,jb} \propto -\frac{1}{2}\{[|\tilde{\psi}_{ia}^{M}(N)|^2 - |\psi_i(N)|^2] + [|\tilde{\psi}_{ia}^{N}(M)|^2 - |\psi_i(M)|^2]\} \quad (12)$$

where in this last equation, it is taken into account that the perturbation has connected the LMO j with vacant b* LMOs at the M nucleus site, in the first bracket, and at the N nucleus site, in the second one. The last two equations lead to the following interpretations of $J_{ia,jb}$: (a) the sum of the contribution of the a*-type vacant LMOs to the electronic density changes of LMO i and the contribution of the b*-type vacant LMOs to LMO j at the site of one nucleus when LMOs j and i are connected with b*-type and a*-type vacant LMOs at the other nucleus, respectively; (b) the sum of the contribution of the a*-type vacant LMOs to the electronic density changes of LMO i at both nuclei sites when LMO j is connected with b*-type vacant LMOs at the other nucleus site.

It is noteworthy that, for long range couplings, due to the local character of LMOs, only one electronic density change contributes significantly to J_{ij} terms in eqs 5 and 6, and to $J_{ia,jb}$ terms in eqs 11 and 12. Therefore, the sign and magnitude of these two and four-indices coupling pathways can be determined by comparing the electronic density of a single perturbed LMO to that of the unperturbed LMO at a particular nucleus site. Taking into account this last observation, it is interesting to note that four-indices coupling pathways can also be calculated as

$$J_{ia,jb} \approx -[|\tilde{\psi}_{ia}^{M}(N)|^2 - |\psi_i(N)|^2] \propto -2\psi_i(N)\delta\tilde{\psi}_{ia}^{M}(N) \quad (13)$$

where $\delta\tilde{\psi}_{ia}^{M}(N)$represents the contribution from vacant LMOs a* to the perturbed $\tilde{\psi}_i^M$. Therefore, $J_{ia,jb}$ is also proportional to the product of the unperturbed i LMO and the vacant a* LMOs.

Localization Technique. The localization technique used in this work is Engelmann's,[12] applied in an iterative way. With this method, occupied and vacant MOs from an ab initio RHF calculation can be transformed to yield LMOs which closely resemble the chemical picture of bonds, lone pairs, inner shells, and their corresponding vacant LMOs (antibonds, anti-lone pairs, etc.). To obtain LMOs, each local fragment is defined by a subset of atomic orbitals (AOs). LMOs within the local fragment are obtained as combinations of MOs with maximun orthogonal projection over the subset of AOs that define the fragment. The only constraint required is that the transformation applied preserves the orthonormality of the LMOs thus obtained (unitary transformation). This procedure is applied separately to occupied and vacant MOs. Occupied LMOs are classified as atom X inner-shells SX, bonding orbitals X−Y (σ and π types), and X atom lone pairs, LPX. In the case of FHF−, there is also an occupied LMO localized mainly in both F atoms, which corresponds to the "extra" electron. This LMO, which will be dubbed F···F, has a particular shape with a predominance of p-character.

The procedure to localize vacant orbitals was fully described in a previous paper.[18] In a similar way as occupied LMOs, vacant LMOs can be classified as follows: (i) The first type is one center vacant LMOs, defined as those having maximun projection on the set of AOs centered at a given nucleus X; they are identified, matching the occupied LMOs classification, as SX* when they are of pure s-type, LPX* when they are of s-p-d-type or LPπX* when they are of pure p-type. (ii) The second type is two-center vacant LMOs, defined between directly bonded atoms; they are identified as X−Y*. As it was explained in a previous paper,[18] in the present application, there are several MOs that could not be localized in this way. They correspond to three-center LMOs localized in the hydrogen bond region F−H···F. This type of vacant LMOs, which could be called "bridge vacant LMOs", arises from vacant canonical MOs of low orbital energies. This fact shows that this type of vacant LMOs are not "supernumerary", but they have a physical sense in the complex formation. These type of vacant LMOs and those of the LPF(A)* type (where 'A' stands for the acceptor F atom) play a fundamental role in the intermolecular coupling transmission. For this reason, these "bridge vacant LMOs" and LPF(A)* ones were joined in a single classification, as HB* vacant LMOs, taking into account that LPF(A)* are also localized in the hydrogen bond zone.

Results and Discussion

Calculations were carried out for the complex FH···FH and FH···F$^-$ for different F···F distances (or, equivalently, different F···H distances). The rest of the molecular geometry was kept without changes. The experimental F···F distance[22] (2.72 Å) for FH···FH was taken as the reference one and it is referred to as the "equilibrium distance". A linear configuration was adopted in order to simplify the analysis, as similar dependence of the coupling with the F···F distance was found for both the linear and the bent dimer.[7] In all cases, atoms and LMOs of the donor molecule are identified with "D" , and those of the acceptor one with "A" . The same geometrical structure was adopted for FH···F$^-$, to facilitate the comparison. Calculations were carried out at the SOPPA and RPA levels by means of the DALTON[23] and SYSMO[24−26] programs, respectively. CLOPPA analysis of J couplings was carried out at the RPA level by means of a modified version of the SYSMO program. Only Fermi contact (FC) terms are considered, as it was shown that this contribution is responsible of the distance dependence of ^{2h}J(F,F).[7] The atomic orbital basis set used is Van Duijneveldt's (13s7p1d,8s1p)-[13s5p1d,5s1p].[27]

Figure 1 shows the distance dependence of the FC terms of (a) ^{1h}J(F,H) and (b) ^{2h}J(F,F), at both RPA and SOPPA levels in FH···FH. It can be seen that correlation effects are important. However, although RPA values of ^{1h}J(F,H) are larger (in absolute value) than SOPPA ones, RPA ones follow similar trends than SOPPA ones. ^{1h}J(F,H) is always negative throughout the distance range shown. Therefore, it can be concluded that RPA values are adequate for performing a qualitative analysis of the distance dependence.

RPA values of ^{2h}J(F,F) show a qualitative trend similar to that seen for the SOPPA ones. There is no monotonic decrease but there is a sign change from positive to negative as the F···F distance increases. Therefore, RPA values are also adequate to perform a qualitative analysis of the distance dependence. Regardless of this fact, there is also a significant difference between RPA and SOPPA graphs. The RPA value of ^{2h}J(F,F) changes sign at a distance larger than equilibrium, while the SOPPA value changes sign at a shorter one. RPA values exhibit the competition of positive and negative effects, consistently with previous results, but numerical agreement with EOM-CCSD values[7] is only found at the SOPPA level. A CLOPPA

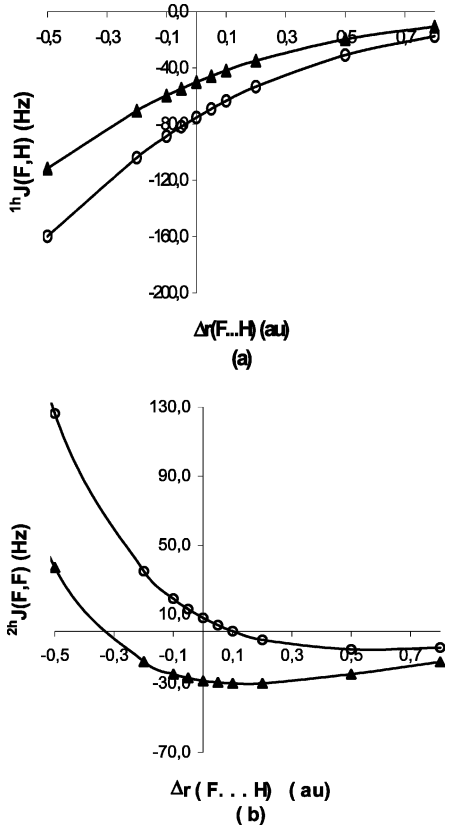

Figure 1. Distance dependence of the FC term of (a) ^{1h}J(F,H), and (b) ^{2h}J(F,F), for linear HF···FH. Δr(F···H) = r(F···H) − r_{eq}(F···H). Key: (▲) SOPPA; (○) RPA.

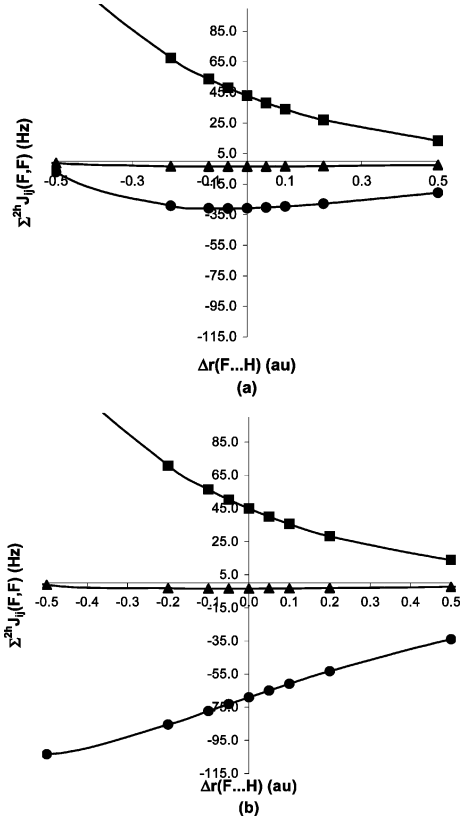

Figure 2. Distance dependence of the sum over i,j indices of $^{2h}J_{ij}$(F,F) coupling pathways: (a) RPA values; (b) corrected RPA values, obtained by rescaling the orbital energy of the LPF(A) LMO as mentioned in the text. Δr(F···H) = r(R···H) - r_{eq}(F···H). Key: (▲) i,j = LMO(D),LMO(D); (●) i,j = LMO(A),LMO(D); (■) i,j = LMO(A),LMO(A). See text for explanation of symbols used.

analysis allows to assess the reason for the sign change of the ^{2h}J(F,F) coupling for increasing F···F distances. It is interesting to remark that, by inspection of the main coupling mechanisms, it is found that by introducing a single fitting parameter (for all distances considered), calculated J values come very close to SOPPA ones. For this reason, this subject will be discussed in first place in the following section. However, as it will be explicitly shown, the qualitative behavior of the different coupling pathways is the same when considering the corrected values obtained when this fitting parameter is introduced, or the original RPA ones. As a consequence, the same conclusions are obtained in both cases.

CLOPPA Analysis of ^{2h}J(F,F) in $(FH)_2$. First, an analysis of the two indices J_{ij} contributions to ^{2h}J(F,F) is carried out. To this end, J_{ij} coupling pathways are grouped taking into account the following criterion: (a) i = occupied LMOs of the acceptor molecule and j = occupied LMOs of the donor molecule (i,j = LMO(A),LMO(D)); (b) both i and j, occupied LMOs of the acceptor molecule (i,j = LMO(A),LMO(A)); (c) both i and j, occupied LMOs of the donor molecule (i,j = LMO(D),LMO(D)). Figure 2a shows the distance dependence of the sum of J_{ij} coupling pathways, grouped as indicated above, calculated at the RPA level.

From Figure 2a it can be seen that the sum of coupling pathways with i,j = LMO(A),LMO(A) shows large positive values while that with i,j = LMO(A),LMO(D) presents negative values of a lesser amount. The sum of coupling pathways with i,j = LMO(D),LMO(D) presents small negative values and it is almost independent of the F···H distance. Therefore, all most significant coupling pathways involve the LMO(A)-type LMOs at least once. Although it can be expected that all LMOs could be affected by correlation effects, it can be thought of that only a few of them are crucial to determine the differences found between SOPPA and RPA ^{2h}J(F,F) values. To achieve a better quantitative agreement between RPA and SOPPA values, the simplest ad hoc correction to RPA ^{2h}J(F,F) values is proposed, involving only the orbital energies. It is based on the following: (a) as it will be shown in the following sections, only a few coupling pathways are relevant to define the coupling, and (b) from them, the sigma lone pair of the acceptor F atom, LPF(A), is the most important one, as it is present in all main coupling pathways at least once. From parts a and b, it could be assumed that a correction of the orbital energy of the canonical MO mostly associated with the LPF(A) LMO could be the most significant one in this case. Thus, a correction factor to this orbital energy is calculated in such a way that ^{2h}J(F,F) at the RPA level matches ^{2h}J(F,F) at the SOPPA level, at the equilibrium distance. Then the same factor is applied to this orbital energy for all distances considered, and ^{2h}J(F,F) is recalculated with this "RPA-like" propagator. The correction factor to the orbital energy is 0.91. Thus, the RPA-like structure of the coupling is preserved but modifying only this particular orbital energy in the calculation of the PP. To sum up, given that one LMO, LPF(A), is involved in all main coupling pathways, the (judicious) supposition that a correction for only this particular LMO may yield adequate corrected ^{2h}J(F,F) coupling is made. Figure 2b shows the distance dependence of the sum of J_{ij} coupling pathways, grouped again as indicated for Figure 2a, considering the "corrected" RPA values. It is interesting to observe, from Figure 2b, that, while terms of the LMO(A),LMO(A)-type are hardly affected by the orbital energy correction, those of the LMO(A),LMO(D)-type become more negative, thus adequately compensating the large positive

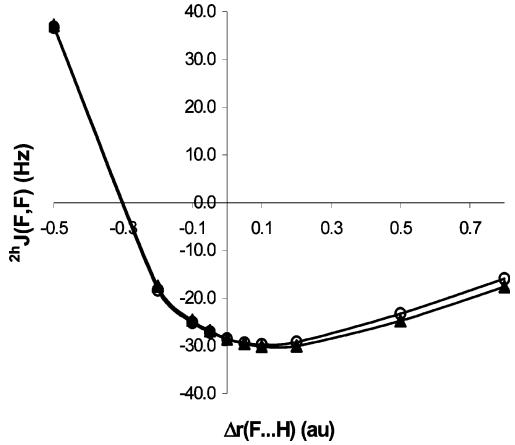

Figure 3. Distance dependence of ^{2h}(J(F,F). Δr(F···H) = r(F···H) − r_{eq}(F···H). Key: (▲) SOPPA; (○) RPA values obtained by rescaling the orbital energy of the LPF(A) LMO as mentioned in the text.

LMO(A),LMO(A)-type terms. The analysis of each individual main $^{2h}J_{ij}$(F,F) coupling pathway shows that the only term that is largely affected by the orbital energy correction is that with i = LPF(A) and j = LPF(D). This positive term changes from 126.08 to 88.27 Hz for the equilibrium distance (ca. 30%), while the other most important terms of this group are nearly unaffected. The sum of LMO(A),LMO(D)-type terms thus becomes ca. 38 Hz more negative.

Finally, Figure 3 depicts the RPA-like values of the FC term of ^{2h}J(F,F) corrected in this way, compared with SOPPA ones.

An exceptionally good agreement is observed between both plots, throughout the range of distances considered. It is worth noting that other attempts to correct different occupied and/or vacant orbital energies do not lead to a good agreement between these RPA-like and SOPPA values. The corrected orbital energy is lower in absolute value than the noncorrected one (−1.4762 au, compared with −1.6209 au, for the reference F···H distance). This fact could be interpreted as correlation increasing the Coulomb interaction more than the exchange interaction between electrons. The result obtained with this simple correction is so exceptionally good that it might deserve further investigation.

In what follows, values obtained considering the corrected orbital energy are considered to carry out the analysis of two and four indices coupling pathways. A comparison with noncorrected RPA values of ^{2h}J(F,F) is also presented. As will be seen, RPA and modified RPA values present the same qualitative behavior and lead to the same conclusions.

Two-Indices $^{2h}J_{ij}$ and Four-Indices $^{2h}J_{ia,jb}$ Contributions. Analysis of the Distance Dependence of the Couplings Signs in $(FH)_2$. ^{2h}J(F,F). The sign change that characterizes the FC term of ^{2h}J(F,F) as a function of distance, was investigated by the NMR triplet wave function model.[7] Here, it is analyzed by means of the CLOPPA method, to give an alternative approach to complement those previous studies. A first insight can be obtained taking into account Figure 2b again. It is worth noting that the sum of terms of the LMO(A),LMO(A)-type is positive, while the sum of terms of the LMO(A),LMO(D)-type is negative. The distance dependence of the former can be rationalized on the following grounds. Both LMOs involved belong to only one of the molecules. Thus, an exponential decrease (in absolute value) can be expected for this type of terms as their contributions depend on the "tails" of occupied LMO(A)-type orbitals at the F(D) nucleus. The distance dependence of LMO(A),LMO(D)-type terms can be analyzed as follows. Each occupied LMO involved ensures a strong magnetic interaction at the corresponding F nucleus position.

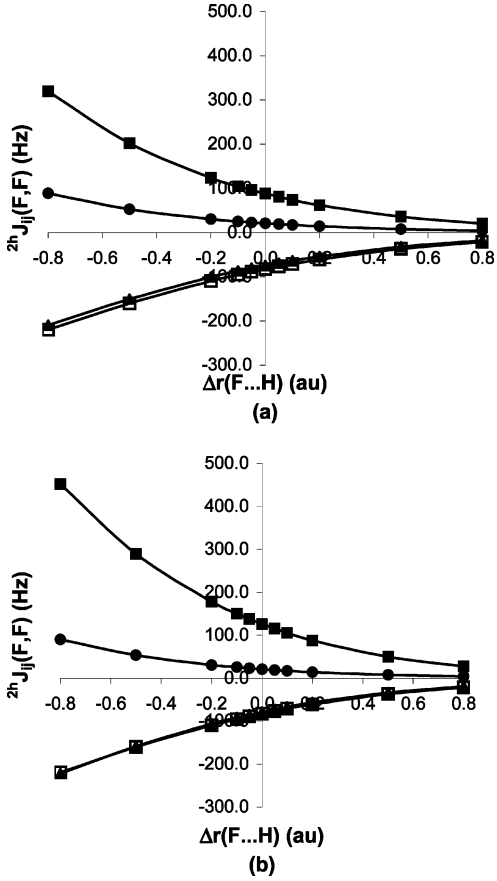

Figure 4. Distance dependence of the main $^{2h}J_{ij}$(F,F) coupling pathways: (a) corrected RPA values; (b) RPA values. Δr(F···H) = r(F···H) − r_{eq}(F···H). Key: (■) i,j = LPF(A),LPF(D); (▲) i,j = LPF(A),F−H(D); (□) i,j = LPF(A),SF(D); (●) i,j = LPF(A),F−H(A). See text for explanation of symbols used.

The distance dependence is determined by the interaction (mostly electrostatic) between LMO(A) and LMO(D). Therefore, an inverse power decrease (in absolute value) can be expected for this type of terms (at least for distances larger than equilibrium). As a consequence, the (positive) sum of LMO(A),LMO(A)-type terms decreases faster than the (negative) sum of LMO(A),LMO(D)-type terms and a negative coupling can be expected as distance increases. However, it must be reminded that, within the sums of terms shown in Figure 2b, different terms may have different signs. Moreover, the question about the reason for the positive or negative sign of each term must be discussed in depth.

Figure 4 shows the distance dependence of the main two-indices coupling pathways $^{2h}J_{ij}$(F,F) (i,j, occupied LMOs) for (a) corrected RPA values, and (b) RPA values.

It can be observed that corrected RPA and RPA values present the same behavior. The only significant difference found is that the LPF(A),LPF(D) corrected terms are smaller than the noncorrected ones, although they show the same dependence with the F···H distance. All terms keep the same sign over the range of distances considered. All main coupling pathways involve the LPF(A) occupied LMO. There are also some less important coupling pathways that involve the F−H(A) LMO. Three terms are the leading ones, namely those which involve LPF(A) with LPF(D), SF(D) and F−H(D), all of them of similar range of magnitude. However, only one of them is positive while the other two terms are negative (+88.27, −82.67, and −74.80 Hz, respectively, for the reference distance), resulting a negative total contribution. The different sign of these terms can be

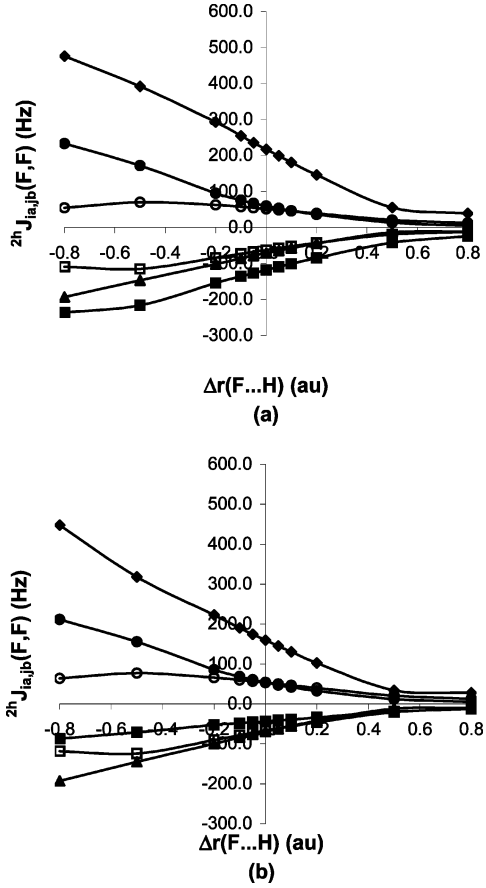

Figure 5. Distance dependence of the main $^{2h}J_{ia,jb}$(F,F) coupling pathways: (a) corrected RPA values; (b) RPA values. Δr(F···H) = r(F···H) − r_{eq}(F···H). i→a*,j→b*: (◆) LPF(A),HB*,LPF(D),LPF(D)*; (■) LPF(A),HB*,LPF(D),HB*; (▲) LPF(A),HB*,SF(D),LPF(D)*; (□) LPF(A),HB*,F−H(D),HB*; (○) LPF(A),HB*,F−H(A),HB*; (●) LPF(A),HB*,LPF(A),HB*. See text for explanation of symbols used.

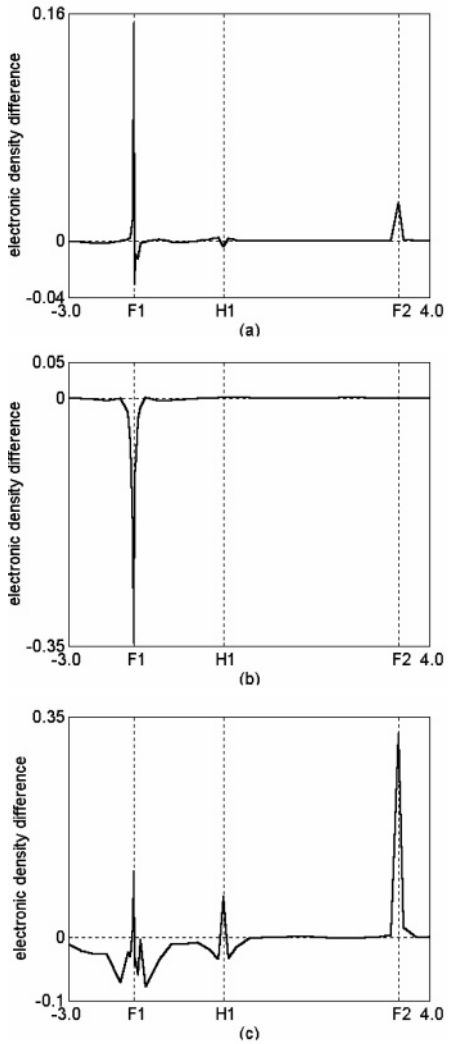

Figure 6. Electronic density difference (in au) between perturbed and unperturbed i LMOs, due to the a* vacant LMO contribution, provided that LPF(A) is connected with HB* vacant LMOs at the F(A) nucleus site: (a) i, a* = LPF(D),HB*; (b) i, a* = LPF(D),LPF(D)*; (c) i, a* = F−H(D),HB*. See text for explanation of symbols used.

interpreted following eq 5. These J_{ij} terms can be thought of as the response of LMOs "i" of the donor molecule due to the magnetic perturbation of LMO "j" = LPF(A) at the F(A) nucleus; i.e., only one electronic density difference of eq 5 is significant. Therefore, a positive J_{ij} indicates that the perturbed LMO i belonging to the F(D) environment, $|\tilde{\psi}_i\rangle$, decreases its electronic density at the F(D) site when LPF(A) is magnetically perturbed at the F(A) nucleus. On the contrary, a negative J_{ij} indicates an electronic density increase of the i LMO. The former is the case of LPF(D), while the latter corresponds to SF(D) and F−H(D). The reason the electronic density of some perturbed LMOs decreases while that of other LMOs increases when LPF(A) is magnetically perturbed can be sought by analyzing the four-indices coupling pathways. Figure 5 depicts the main four-indices coupling pathways over the whole range of distances considered for both corrected and noncorrected RPA values.

Again, corrected and noncorrected RPA values present the same dependence with the F···H distance. The only significant differences are the larger corrected LPF(A),HB*,LPF(D), LPF(D)* term compared to the noncorrected one, and the corrected LPF(A),HB*,LPF(D),HB*, which is more negative than the noncorrected one. The change of only these two terms leads to the exceptionally good agreement between corrected RPA and SOPPA values. All main $^{2h}J_{ia,jb}$(F,F) values do not change sign over the whole range of distances. Thus, the sign change is due to the competition of negative and positive contributions. Bearing in mind the interpretation of four-indices coupling pathways, eq 11, and that each occupied LMO usually belongs to the electronic environment of only one nucleus, the sign of $J_{ia,jb}$ can be explained as follows. The j LMO is magnetically perturbed and connected with the b* vacant LMO at one nucleus site. A positive (negative) $J_{ia,jb}$ value indicates a decrease (increase) of the electronic density of the perturbed i LMO at the site of the other nucleus, when compared to the unperturbed LMO, due to the a* vacant LMO contribution. It is interesting to observe that all main coupling pathways involve the virtual excitation $j \rightarrow b^*$ = LPF(A) → HB* at least once. This characteristic was observed and explained in a previous paper.[18] Thus, all these coupling pathways can be thought of as the response of the electronic system to the magnetic perturbation connecting LPF(A) with HB* at the F(A) nucleus site. Figure 6 shows the density changes $|\tilde{\psi}_{ia}|^2 - |\psi_i|^2$ for the three largest $J_{ia,jb}$ terms in Figure 5.

As mentioned above, the electronic density difference at the F(D) site shows the magnitude and the (inverse) sign of each four-indices coupling pathway considered. The positive or negative sign (and thus, the sign of the $J_{ia,jb}$ as well) can be rationalized as follows. When a given "j" LMO is magnetically perturbed at the F(A) nucleus site and connected to a vacant "b*" LMO, the distribution of electronic charge within the

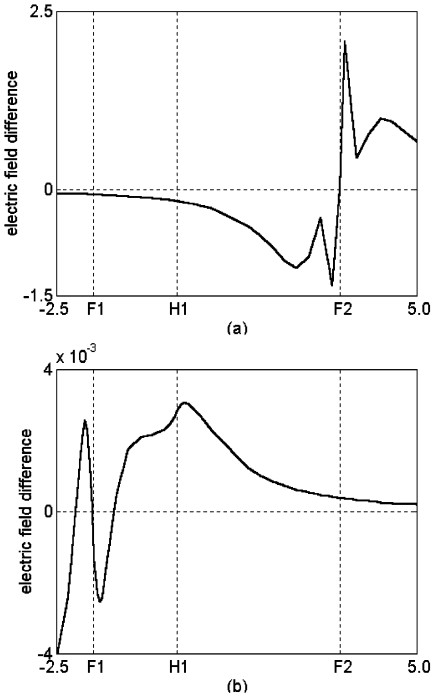

Figure 7. Plot of the electric field change (in au) of the *j* LMO, as it is magnetically perturbed and connected with the HB* vacant LMO, at the F(A) nucleus site: (a) j = LPF(A); (b) j = F−H(D). See text for explanation of symbols used.

molecule is altered. As a result, the mean electric field on electrons occupying other LMOs is changed. In fact, the polarization propagator describes this internal change, thus determining the sign and magnitude of the "response" $i \rightarrow a^*$. However, when a dominant mechanism operates, this change can be explained on qualitative grounds. In the present case, it is interesting to observe that, as j = LPF(A) is connected with b^* = HB* vacant LMOs, it can be expected that it becomes more spread over the whole bridge region. As a consequence, the electric field around the F(A) nucleus changes its intensity in such a way that it favors the electronic charge flow toward it. Figure 7a shows this electric field change. Therefore, the perturbed ĩ LMO tends to increase its density at the F(A) nucleus site, if it is connected with vacant "a^*" LMOs which extend toward the F(A) site. This is the case of the HB* contribution to the perturbed LPF(D) (Figure 6a) and F−H(D) (Figure 6c), LMOs in which density changes seem to be affected by this electric field. However, it must be noted, following eq 13, that the density change shape of the a^*-contribution of the perturbed LMO resembles the product of the unperturbed LMO and the a^* vacant LMOs under consideration. This product determines uniquely the relative signs at F(D) and F(A) of the $i \rightarrow a^*$ density change. Therefore, a positive density change in F(A) determines unambiguously a positive change in F(D) in the case of the HB* contribution to perturbed LPF(D) (Figure 6a) and F−H(D) (Figure 6c).

Figure 6b deserves a similar analysis. However, it can be noted that the LPF(D)* contribution to the perturbed LPF(D) LMO does not allow this LMO to have a contribution at the F(A) site. Thus, it is not affected by the perturbed LPF(A) electric field, but by another "more local" electric field. Figure 7b shows, for instance, the electric field change of the j = F−H(D) LMO as it is magnetically perturbed and connected with the b^* = HB* vacant LMO, at the F(A) nucleus site. This electric field favors a decrease of electronic density around the F(D) site and, therefore, it can be responsible of the a^* = LPF(D)* contribution to the decrease of the perturbed i = LPF(D) electronic density.

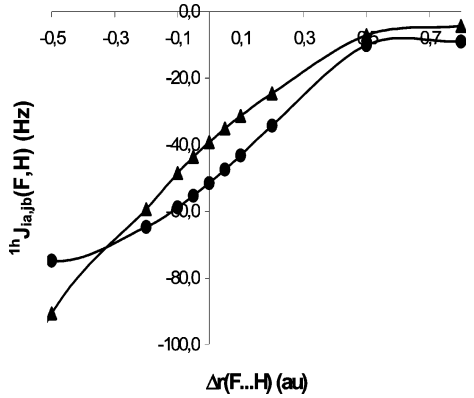

Figure 8. Distance dependence of the main $^{1h}J_{ia,jb}$(F,H) coupling pathways. Δr(F···H) = r(F···H) − r_{eq}(F···H). $i \rightarrow a^*, j \rightarrow b^*$: (●) LPF(A),HB*,F−H(D),HB*; (▲) LPF(A),HB*,F−H(D),F−H(D)*. See text for explanation of symbols used.

^{1h}J(F,H). As it was already mentioned, ^{1h}J(F,H) does not change its sign throughout the range of F···H distances considered. This behavior, opposite to that of ^{2h}J(F,F), can be easily understood following a similar analysis to that of the preceding section. It is remarkable that the whole coupling is due to only two four-indices coupling pathways, namely, those which involve the LPF(A) → HB* excitation with F−H(D) → HB* and F−H(D) → F−H(D)* excitations. Figure 8 shows the distance dependence of these two $J_{ia,jb}$ terms, which are both negative for all distances considered.

To explain the sign of these coupling pathways, the same considerations than for ^{2h}J(F,F) can be applied. We consider the magnetic perturbation producing the LPF(A) → HB* ($j \rightarrow b^*$) excitation. As mentioned above, this causes a field in the F(A) surrounding which favors an increase of electronic density. However, the shape of the F−H(D) → HB* ($i \rightarrow a^*$) contribution to ĩ is independent of the perturbation, and it is shown in Figure 6c. Therefore, an increase of density at F(A) implies a positive contribution of the F−H(D) → HB* ($i \rightarrow a^*$) excitation to the coupling. In turn, this implies necessarily a positive contribution at H(D) as well, thus determining a negative $J_{ia,jb}$ value. The case F−H(D) → F−H(D)* ($i \rightarrow a^*$) can be rationalized on the same grounds. The field shown in Figure 7a due to the LPF(A) → HB* ($j \rightarrow b^*$) excitation favors an increase of electronic density at the H(D) nucleus, i.e., a negative $J_{ia,jb}$ coupling pathway.

Summing up, the sign of the main coupling pathways defining ^{1h}J(F,H) can be rationalized to be negative by analyzing the perturbed ĩ LMO density change in terms of the internal field change caused by the $j \rightarrow b^*$ excitation.

CLOPPA Analysis of ^{2h}J(F,F) in FHF$^-$. Figure 9 shows the distance dependence of the FC term of ^{2h}J(F,F) in FH···F$^-$.

^{2h}J(F,F) is positive and large throughout the range of distances considered. It can be seen that it presents the characteristic exponential decay, a behavior that is quite different from the preceding analyzed one, for ^{2h}J(F,F) in the FH···FH dimer. To investigate the source of this different behavior, main two-indices coupling pathways are considered. Figure 10 displays the principal J_{ij} coupling pathways vs the F···H distance.

From Figure 10, it can be seen that the main $^{2h}J_{ij}$(F,F) coupling pathways have the same sign than the corresponding ones in FH···FH (cf. Figure 4) and keep the same sign over the range of distances considered. However, the comparison of

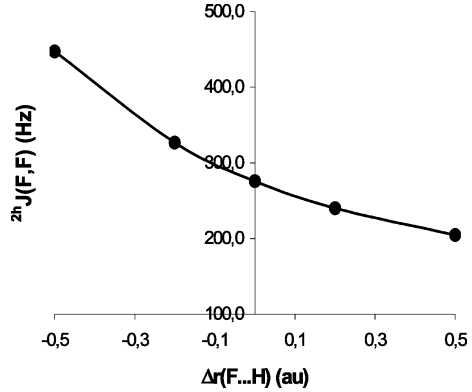

Figure 9. Distance dependence of the FC term of ^{2h}J(F,F) for HF···F−. Δr(F···H) = r(F···H) − r_{eq}(F···H).

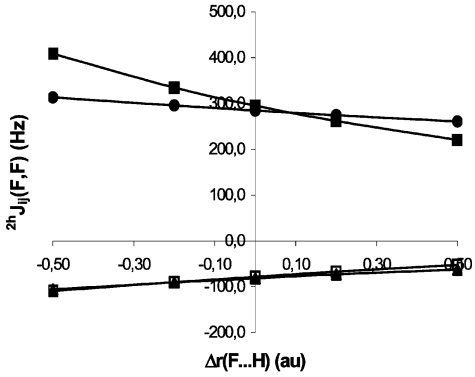

Figure 10. Distance dependence of the main $^{2h}J_{ij}$(F,F) coupling pathways in FH···F−. Δr(F···H) = r(F···H) − r_{eq}(F···H): (■) i,j = LPF(A),LPF(D); (▲) i,j = LPF(A),F−H(D); (□) i,j = LPF(A),SF(D); (●) i,j = LPF(A),F(D)···F(A). See text for explanation of symbols used.

similar coupling pathways in both complexes shows that there are several features that are responsible of the differences between both cases:

(1) Although the term involving the F−H(A) and the LPF(A) LMOs, which is positive and rather important in $(FH)_2$ is not present in FHF^-, there is a larger contribution arising from the F···F LMO, namely, the LPF(A),F···F coupling pathway (284.55 Hz for the reference distance; cf. with 20.75 Hz for ij = LPF(A),F−H(A) in $(FH)_2$).

(2) While negative contributions like LPF(A),F−H(D) and LPF(A),SF(D) are similar in magnitude like the corresponding ones in FH···FH, the most important positive one, LPF(A),LPF(D) is larger for FHF^- than for $(FH)_2$ (295.20 and 88.27 Hz, respectively for the reference distance).

The first point can be understood taking into account that the F···F occupied LMO is a rather delocalized one, due to the extra electron yielding an overall negative charge. Thus, its orbital energy (that is, the orbital energy of the canonical MO mostly associated with it) is high (−0.1271 au; cf., for example, with −0.8034 au, for F−H(A) in $(FH)_2$), and this fact favors the virtual excitations. For example, the four-indices coupling pathway $J_{ia,jb}$ with ia,jb = LPF(A),HB*,F···F,HB* is the largest one (402.31 Hz).

The second point can be rationalized by inspection of the four-indices coupling pathways. Lets take, for example the reference distance. The main $J_{ia,jb}$ which include the occupied LMOs LPF(A) and LPF(D) are, in the case of $(FH)_2$, those which involve the virtual excitations LPF(A) → HB*, LPF(D) → LPF(D)*, and LPF(A) → HB*, LPF(D) → HB*. These two terms are opposite in sign (+217.38 and −117.81 Hz, respectively), and therefore, they partially cancel each other. In the case of FHF^-, there is nearly no cancellation, as these two terms are +332.23 and −12.45 Hz, respectively. It is seen that the negative term which involves the virtual excitations LPF(A) → HB*, LPF(D) → HB* is significantly smaller in FHF^- than in $(FH)_2$. By inspection of the corresponding perturbators and PP elements (see eq 1), it can be seen that, while the former are similar in both cases, the latter are considerable smaller in FHF^- than in $(FH)_2$. This fact can be explained on the following grounds. As it was precedingly mentioned, vacant LMOs of the HB* type, which are most important, are linear combinations of vacant canonical MOs of low energy. The orbital energies of the first vacant canonical MOs of the $(FH)_2$ dimer are 0.0722 (LUMO), 0.1692, and 0.3791 au, while, the LUMO of the FHF^- has an orbital energy of 0.3517 au. This means that some virtual excitations to HB* vacant LMOs are less favorable in FHF^- than in $(FH)_2$, yielding PP elements that are smaller in the former than in the latter. For example, if the LUMO energy in FHF^- is lowered to 0.2 au, the term which involves the LPF(A) → HB*, LPF(D) → HB* virtual excitations increases from −12.45 to −63.49 Hz.

Concluding Remarks

The CLOPPA decomposition of J couplings in contributions of local fragments led to an explanation of the behavior of ^{2h}J(F,F) and ^{1h}J(F,H) as a function of the F···H distance, in the $(FH)_2$ dimer, and to understand the differences from the expected exponential decrease that presents, for example, the same coupling in FHF^-. The use of LMOs allows an analysis of coupling mechanisms in terms of a few main "two- and four-indices coupling pathways". The change of sign of ^{2h}J(F,F) as the F···H distance increases is due to the competition of mean positive LMO(A),LMO(A) and mean negative LMO(A),LMO(D) contributions. The first ones dominate at short distances, but decrease in magnitude more rapidly than the second ones. This trends can be explained taking into account that LMO(A),LMO(A) contributions depend on the "tails" of occupied LMO(A)-type orbitals and the shape of the vacant LMOs. Thus, an exponential decrease (in absolute value) for this type of terms can be expected. This is not the case of LMO(A),LMO(D)-type contributions, which depend on the interaction (mostly electrostatic) between LMO(A) and LMO(D). Therefore, an inverse power decrease (in absolute value) is expected. The sign of different individual coupling pathway $J_{ia,jb}$ was rationalized in terms of the density of the magnetically perturbed LMOs: (i) the $j \rightarrow b^*$ density change induced by the magnetic perturbation is calculated; (ii) the change in the mean field on the rest of the electronic distribution caused by this density change is obtained; (iii) the sign of the $i \rightarrow a^*$ contribution is rationalized by analyzing what density change of the i LMO is favored by the field in part ii. Strictly speaking, such sign depends on all Coulomb and exchange interactions as contained in the polarization propagator of the system. However, it was shown that in the present case it can be anticipated by qualitative physical considerations. This approach thus provides an intuitive insight that can be extrapolated to other phenomena under similar conditions and, in that sense, it can be considered as predictive.

Acknowledgment. Financial support from UBACYT and CONICET is gratefully acknowledged. We would like to thank Prof. P. Lazzeretti for providing us a copy of the SYSMO program.

References and Notes

(1) Rae, I. D.; Weigold, J. A.; Contreras, R. H.; Biekofsky, R. R. *Magn. Reson. Chem.* **1993**, *31*, 836.

(2) Dingley, A. J.; Grzesiek, S. *J. Am. Chem. Soc.* **1998**, *120*, 8293. Dingley, A. J.; Masse, J. E.; Peterson, R. D.; Barfield, M.; Feigon, J.; Grzesiek, S. *J. Am. Chem. Soc.* **1999**, *121*, 6019.

(3) Fukui, H.; Baba, T. *Specialist Periodical Reports: Nuclear Magnetic Resonance*; Royal Society of Chemistry: London, 2000; Vol. 30, p 109 and references therein.

(4) Kamienska-Trela, K.; Wojcik, J. *Specialist Periodical Reports: Nuclear Magnetic Resonance*; Royal Society of Chemistry: London, 2002; Vol. 32, p 181 and references therein.

(5) Alkorta, I.; Elguero, J. *Int. J. Mol. Sci.* **2003**, *4*, 64, and references therein.

(6) Kamienska-Trela, K.; Wojcik, J. *Specialist Periodical Reports: Nuclear Magnetic Resonance*; Royal Society of Chemistry: London, 2005; Vol. 34, p 196 and references therein.

(7) Del Bene, J. E.; Elguero, J.; Alkorta, I.; Yáñez, M.; Mó, O. *J. Chem. Phys.* **2004**, *120*, 3237.

(8) Pecul, M.; Sadlej, J.; Leszczynski, J. *J. Chem. Phys.* **2001**, *115*, 5498.

(9) Del Bene, J. E.; Elguero, J. *Chem. Phys. Lett.* **2003**, *382*, 100.

(10) Engelmann, A. R.; Contreras, R. H. *Int. J. Quantum Chem.* **1983**, *23*, 1033.

(11) Ruiz de Azúa, M. C.; Diz, A. C.; Giribet, C. G.; Contreras, R. H.; Rae, I. D. *Int. J. Quantum Chem.* **1986**, *S20*, 585.

(12) Diz, A. C.; Giribet, C. G.; Ruiz de Azúa, M. C.; Contreras, R. H. *Int. J. Quantum Chem.* **1990**, *37*, 663.

(13) Ruiz de Azúa, M. C.; Giribet, C. G.; Vizioli, C. V.; Contreras, R. H. *J. Mol. Struct. (THEOCHEM)* **1998**, *433*, 141.

(14) Giribet, C. G.; Ruiz de Azúa, M. C.; Gómez, S. B.; Botek, E. L.; Contreras, R. H.; Adcock, W.; Della, E. W.; Krstic, A. R.; Lochert, I. J. *J. Comput. Chem.* **1998**, *19*, 181.

(15) Giribet, C. G.; Demarco, M. D.; Ruiz de Azúa, M. C.; Contreras, R. H. *Mol. Phys.* **1997**, *91*, 105.

(16) Lazzeretti, P.; Malagoli, M.; Zanasi, R.; Della, E. W.; Lochert, I. J.; Giribet, C. G.; Ruiz de Azúa, M. C.; Contreras, R. H. *J. Chem. Soc., Faraday Trans.* **1998**, *91*, 4031.

(17) Giribet, C. G.; Ruiz de Azúa; M. C.; Vizioli, C. V.; Cavasotto, C. N. *Int. J. Mol. Sci.* **2003**, *4*, 203.

(18) Giribet, C. G.; Ruiz de Azúa; M. C. *J. Phys. Chem. A* **2005**, *109*, 11980.

(19) Jørgensen, P.; Simons, J. *Second Quantization-Based Methods in Quantum Chemistry*; Academic Press: London; 1981.

(20) Geertsen, J.; Oddershede, J. *Chem. Phys.* **1984**, *90*, 301.

(21) Enevoldsen, T.; Oddershede, J.; Sauer, S. P. A. *Theor. Chim. Acc.* **1998**, *100*, 275.

(22) Howard, B. J.; Dyke, T. R.; Klemperer, W. *J. Chem. Phys.* **1984**, *81*, 5417 (*Gaussian 98, Revision A.7* Frisch, M. J.; Trucks, G. W.; Schlegel, H. B.; Scuseria, G. E.; Robb, M. A.; Cheeseman, J. R.; Zakrzewski, V. G.; Montgomery, J. A.; Stratmann, R. E., Jr.; Burant, J. C.; Dapprich, S.; Millam, J. M.; Daniels, A. D.; Kudin, K. N.; Strain, M. C.; Farkas, O.; Tomasi, J.; Barone, V.; Cossi, M.; Cammi, R.; Mennucci, B.; Pomelli, C.; Adamo, C.; Clifford, S.; Ochterski, J.; Petersson, G. A.; Ayala, P. Y.; Cui, Q.; Morokuma, K.; Malick, D. K.; Rabuck, A. D.; Raghavachari, K.; Foresman, J. B.; Cioslowski, J.; Ortiz, J. V.; Baboul, A. G.; Stefanov, B. B.; Liu, G.; Liashenko, A.; Piskorz, P.; Komaromi, I.; Gomperts, R.; Martin, R. L.; Fox, D. J.; Keith, T.; Al-Laham, M. A.; Peng, C. Y.; Nanayakkara, A.; Gonzalez, C.; Challacombe, M.; Gill, P. M. W.; Johnson, B.; Chen, W.; Wong, M. W.; Andres, J. L.; Gonzalez, C.; Head-Gordon, M.; Replogle, E. S.; Pople, J. A. Gaussian, Inc.: Pittsburgh, PA, 1998.

(23) DALTON, a Molecular Electronic Structure Program, Release 1.2: Helgaker, T.; Jensen, H. J. Aa.; Jørgensen, P.; Olsen, J.; Ruud, K.; Ågren, H.; Auer, A. A.; Bak, K. L.; Bakken, V.; Christiansen, O.; Coriani, S.; Dahle, P.; Dalskov, E. K.; Enevoldsen, T.; Fernandez, B.; Hättig, C.; Hald, K.; Halkier, A.; Heiberg, H.; Hettema, H.; Jonsson, D.; Kirpekar, S.; Kobayashi, R.; Koch, H.; Mikkelsen, K. V.; Norman, P.; Packer, M. J.; Pedersen, T. B.; Ruden, T. A.; Sanchez, A.; Saue, T.; Sauer, S. P. A.; Schimmelpfennig, B.; Sylvester-Hvid, K. O.; Taylor, P. R.; Vahtras, O. 2001.

(24) Lazzeretti, P.; Zanasi, R. *J. Chem. Phys.* **1982**, *77*, 2448.

(25) Lazzeretti, P. *Int. J. Quantum Chem.* **1979**, *15*, 181.

(26) Lazzeretti, P. *J. Chem. Phys.* **1979**, *71*, 2514.

(27) Van Duijneveldt, F. B. *IBM Res. Rep.* **1971**, RJ 945.